

SREBP-2-deficient and hypomorphic mice reveal roles for SREBP-2 in embryonic development and SREBP-1c expression^S

Laurent Vergnes,* Robert G. Chin,* Thomas de Aguiar Vallim,[†] Loren G. Fong,[†] Timothy F. Osborne,[§] Stephen G. Young,^{*,†,***} and Karen Reue^{1,*,†,***}

Departments of Human Genetics* and Medicine,[†] David Geffen School of Medicine at the University of California, Los Angeles, CA 90095; Metabolic Disease Program,[§] Sanford-Burnham Medical Research Institute, Orlando, FL 32827; and Molecular Biology Institute,^{**} University of California, Los Angeles, CA 90095

Abstract Cholesterol and fatty acid biosynthesis are regulated by the sterol regulatory element-binding proteins (SREBPs), encoded by *Srebf1* and *Srebf2*. We generated mice that were either deficient or hypomorphic for SREBP-2. SREBP-2 deficiency generally caused death during embryonic development. Analyses of *Srebf2*^{-/-} embryos revealed a requirement for SREBP-2 in limb development and expression of morphogenic genes. We encountered only one viable *Srebf2*^{-/-} mouse, which displayed alopecia, attenuated growth, and reduced adipose tissue stores. Hypomorphic SREBP-2 mice (expressing low levels of SREBP-2) survived development, but the female mice exhibited reduced body weight and died between 8 and 12 weeks of age. Male hypomorphic mice were viable but had reduced cholesterol stores in the liver and lower expression of SREBP target genes. Reduced SREBP-2 expression affected SREBP-1 isoforms in a tissue-specific manner. In the liver, reduced SREBP-2 expression nearly abolished *Srebf1c* transcripts and reduced *Srebf1a* mRNA levels. In contrast, adipose tissue displayed normal expression of SREBP target genes, likely due to a compensatory increase in *Srebf1a* expression. Our results establish that SREBP-2 is critical for survival and limb patterning during development. **■** Reduced expression of SREBP-2 from the hypomorphic allele leads to early death in females and reduced cholesterol content in the liver, but not in adipose tissue.—Vergnes, L., R. G. Chin, T. de Aguiar Vallim, L. G. Fong, T. F. Osborne, S. G. Young, and K. Reue. **SREBP-2-deficient and hypomorphic mice reveal roles for SREBP-2 in embryonic development and SREBP-1c expression.** *J. Lipid Res.* 2016. 57: 410–421.

Supplementary key words sterol regulatory element-binding protein 2 • sterol regulatory element-binding protein 1c • gene regulation • cholesterol synthesis

This work was supported by the Public Health Service P01 HL90553 (S.G.Y., L.G.F., K.R.) and U01 HL66621 Program in Genomics Applications (S.G.Y., K.R.), and American Heart Association 14SDG18440015 (T.A.V.).

Manuscript received 29 September 2015 and in revised form 15 December 2015.

Published, JLR Papers in Press, December 18, 2015

DOI 10.1194/jlr.M064022

Cholesterol is a precursor for the biosynthesis of steroid hormones, bile acids, and vitamin D, and is a critical determinant of cell membrane permeability and fluidity (1, 2). Cholesterol biosynthesis and homeostasis are regulated by the sterol regulatory element-binding protein (SREBP) transcription factor family. SREBPs are basic-helix-loop-helix-leucine zipper transcription factors, which are activated in response to low cellular sterol levels by a series of protein cleavage/transport events (3–5). There are three SREBP isoforms, which originate from two genes. *Srebf1* encodes SREBP-1a and SREBP-1c, which have distinct promoters and 5' exons. *Srebf2* encodes SREBP-2. SREBP-1c is the predominant isoform in metabolic tissues such as liver and adipose tissue, but has a relatively weak transcription-activation domain compared with the other SREBPs. There is overlap in the activities of the SREBP isoforms, but it is generally held that SREBP-1c primarily targets genes implicated in fatty acid synthesis, whereas SREBP-2 preferentially regulates genes involved in cholesterol synthesis (5–8). SREBP-1a is a potent activator of both triglyceride and cholesterol biosynthetic pathways, but is expressed at low levels in metabolic tissues, making the physiological role of the protein unclear (9). SREBP-1c, itself, is regulated by SREBPs, indicating a high degree of cross-talk among SREBP proteins, making it difficult to assign distinct physiological functions to individual SREBP proteins.

Abbreviations: *Acc*, acetyl-CoA carboxylase; AER, apical ectodermal ridge; BMP, bone morphogenetic protein; FGF, fibroblast growth factor; *Grem1*, gremlin 1; *Hmgcr*, HMG-CoA reductase; *Hmgcs*, HMG-CoA synthase; *Insig*, insulin-induced protein; *Ldlr*, LDL receptor; MEF, mouse embryonic fibroblast; *Ptch1*, patched 1; SCAP, SREBP cleavage-activating protein; *Scd1*, stearoyl-CoA desaturase 1; SHH, sonic hedgehog; SREBP, sterol regulatory element-binding protein; WAT, white adipose tissue; ZPA, zone of polarizing activity.

¹To whom correspondence should be addressed.

e-mail: reuek@ucla.edu

^SThe online version of this article (available at <http://www.jlr.org>) contains a supplement.

SREBP activity is regulated by the nutritional status of the cell (10, 11). When cellular sterol concentrations are high, SREBP precursors are bound to SREBP cleavage-activating protein (SCAP) in the endoplasmic reticulum membrane. SCAP, in turn, interacts with insulin-induced proteins (Insigs), which serve to retain the SCAP-SREBP complex within the endoplasmic reticulum membrane. When sterol concentrations are low, SCAP-bound SREBPs are translocated to the Golgi where they undergo a two-step cleavage process (by S1P and S2P proteases), thereby releasing the N-terminal active domain (nuclear SREBP).

Studies with genetically modified mice have provided insight into the physiological roles of the three SREBP isoforms [reviewed in (3, 5)]. The characterization of transgenic mice with expression of constitutively active nuclear forms of SREBP-1a, -1c, or -2 led to the identification of preferential target genes for SREBP-1 (lipogenesis genes) and SREBP-2 (cholesterol synthetic genes) (9, 12, 13). However, the physiological roles of the SREBP proteins cannot be fully delineated with constitutively active transgenes that lack the capacity to be regulated by sterols. Studies with gene knock-out models have largely confirmed the gene targets for SREBP-1 and have provided additional insights into the physiological roles of this protein. Because of the critical functions of the SREBP pathway, SREBP-1 deficiency is lethal in utero in 50–85% of mice (14). Although no analysis of SREBP-2-deficient mice has been published, Shimano et al. (14) did comment that SREBP-2 deficiency is lethal during embryogenesis. Also, deficiency in S1P, which is required for activation of all SREBP isoforms, is lethal in utero (15). SCAP and S1P function has been examined with conditional gene knockouts in liver, which revealed marked (70–80%) reductions in hepatic cholesterol and fatty acid levels (15, 16).

Although the SREBP-1, S1P-, and SCAP-deficient mice have revealed the importance of the SREBP pathway during embryogenesis, the role of each protein during development has not been studied in detail. It is intuitive that lipid homeostasis should be critical for normal development, because upregulation of cholesterol and phospholipid synthesis is required to satisfy the demand for membrane biogenesis during periods of rapid cell proliferation. Also, it is well-documented that impaired sterol synthesis results in developmental defects in humans and animals (17–20). However, the activities of SREBP-1 and SREBP-2 that make them indispensable for development have not been identified. In the current study, we set out to elucidate the physiological role of SREBP-2 during embryonic development and in the liver and adipose tissue of adult mice. Both of these objectives were approachable after identifying a gene-trap allele for *Srebf2*. That mutant allele made it possible to generate both SREBP-2-deficient mice and hypomorphic SREBP-2 mice.

MATERIALS AND METHODS

Generation of mutant mice

Mouse embryonic stem cells containing a gene-trap insertion in *Srebf2* (cell line XD155) were obtained from BayGenomics

(now <http://www.genetrap.org>) (21, 22). Insertion of the gene-trap vector pGT1Lxf into *Srebf2* was verified by direct sequencing of cDNA obtained by 5' rapid amplification of cDNA ends (5'-RACE). Male chimeric mice from blastocyst microinjections were then bred with C57BL/6J females to generate mice carrying the mutant *Srebf2* allele. The site of the gene-trap insertion within intron 1 of the *Srebf2* gene was determined by inverse PCR. Offspring were genotyped by PCR of genomic DNA with primers specific for the WT *Srebf2* allele (5'-tgaaactgcggatcaggctgg-3', 5'-gctggatccctggagttac-3'; 483 bp) and for the mutant allele carrying the insertional mutation (5'-gatgccagactcagtgaag-3', 5'-gctgcaaggcggatgaattgg-3'; 482 bp). To generate *Srebf2* hypomorphic mice, *Srebf2*^{+/-} mice were crossed with an *Hprt-Cre* transgenic mouse (23). The Cre-mediated recombination event eliminated the floxed splice acceptor site in the gene-trapped allele; recombination was detected by a shift in the size of the PCR product generated from the mutant allele (from 482 to 136 bp). The *Cre* transgene was detected by PCR (primers 5'-accagccagctatcaactcg-3', 5'-ttacattggctcagccacc-3'; 199 bp). Mice were housed in a 12 h light/dark cycle and fed a Purina 5001 chow diet. Samples were collected around 1:00 PM, after 5 h fasting. Mouse studies were performed under approval from the University of California at Los Angeles Institutional Animal Care and Use Committee.

Tissue staining and histology

Fresh tissues were fixed in 4% paraformaldehyde and then processed as described (24). Tissues and embryos were stained for β -galactosidase expression, as described (25) with minor modifications. Tissue samples were directly embedded in OCT (Sakura Finetek) and frozen. Fresh 10 μ m sections were fixed with 2% formaldehyde and 0.2% glutaraldehyde in PBS for 5 min and incubated in X-gal solution at 37°C overnight. For whole embryos, samples were fixed in 4% paraformaldehyde for 5 min, washed three times in PBS, and stained. Skeletal staining was performed with Alizarin red and Alcian blue as described (www.hhmi.ucla.edu/derobertis/).

Whole mount in situ hybridization

Mouse in situ hybridization on whole mounts was performed as described (www.hhmi.ucla.edu/derobertis/). The probes were described previously (26–28).

Cell culture and cholesterol depletion

Mouse embryonic fibroblasts (MEFs) were prepared from embryos harvested 11.5 days post coitus. Cells were maintained at 37°C in 5% CO₂ with DMEM containing 10% FBS, penicillin/streptomycin, 1 mM pyruvate, 2 mM glutamine, and nonessential amino acids. Cells were immortalized by continuous passaging. For cholesterol-depletion studies, MEFs were plated on 12-well plates (100,000 cells/well) on day 1. On day 2, the cells were treated overnight with DMEM containing 10% charcoal-stripped FBS (Gibco, 12676-011), 0.5% (2-hydroxypropyl)- β -cyclodextrin (Sigma, C0926), and 20 μ M mevastatin (Tocris, 1526). The same results were obtained with two independent WT and *Srebf2*^{-/-} cell lines.

Gene expression analyses

Total RNA was isolated from mouse tissues and MEFs by extraction with TRIzol (Invitrogen). cDNA synthesis, RT-PCR, and quantitative (q)PCR were performed as described (24). Gene expression was normalized to β 2 microglobulin and 36b4. All primer sequences used in this study are presented in supplementary Table 1. Relative miR-33a expression was determined by TaqMan RT-PCR using a predesigned probe set (Applied Biosystems)

from cDNA synthesized from 100 ng total RNA (Applied Biosystems) and normalized to SnoRNA 202.

Western blot analyses

Livers were rinsed in cold PBS and homogenized in buffer A [10 mM HEPES (pH 7.4), 0.42 M NaCl, 2.5% glycerol, 1.5 mM MgCl₂, 0.5 mM Na-EDTA, 0.5 mM EGTA]. Nonhomogenized tissue was removed with a 100 μm cell strainer, and the homogenate was centrifuged at 4,000 rpm for 15 min at 4°C. The supernatant fluid was centrifuged again at 13,000 rpm for 10 min at 4°C. The resulting pellet was resuspended in buffer B (buffer A containing 100 mM NaCl) to generate the cytosolic fraction. The original pellet was resuspended in buffer C [10 mM HEPES (pH 7.4), 0.42 M NaCl, 2.5% glycerol, 1.5 mM MgCl₂, 0.5 mM Na-EDTA, 0.5 mM EGTA]. Twenty micrograms of these fractions were used for Western blot studies. Protein visualization was performed with rabbit anti-mouse SREBP-2 antibodies [1:5,000 (29)] followed by an HRP-conjugated goat anti-rabbit IgG (1:20,000), and detected with an ECL+ kit (GE Healthcare).

Lipid analysis

For tissue lipid analysis, samples were processed as described (24). Total proteins were quantified for normalization between samples (BCA kit, Pierce).

Steroid hormone quantification

Plasma hormones were determined by the Endocrine Support Core Lab at Oregon National Primate Research Center.

RESULTS

SREBP-2 is required for viability and for limb bud development during mouse embryogenesis

To generate mouse models with absent or reduced SREBP-2, we used a gene-trap allele containing an insertional mutation in intron 1 of *Srebf2*. The transcript from this allele contains exon 1 of *Srebf2* joined in-frame to a β-geo cassette (a fusion of a *lacZ* and a neomycin phosphotransferase gene) (Fig. 1A). The resulting SREBP-2-β-geo fusion protein contains only the first 29 amino acids of SREBP-2; it lacks 97% of the SREBP-2 sequences, including those encoding the DNA-binding and transmembrane domains (Fig. 1B). *Srebf2*^{+/−} mice appeared normal; *Srebf2*^{−/−} mice died in utero, aside from a single live birth (described later). This is in agreement with Shimano et al. (14), who commented that *Srebf2* knockout mice die during embryogenesis (although the embryos were not further characterized).

To assess SREBP-2 expression during embryogenesis, we examined *Srebf2*^{+/−} embryos for β-galactosidase expression, which is controlled by the endogenous *Srebf2* regulatory elements. High levels of *Srebf2* expression were observed throughout embryogenesis (Fig. 1C). At embryonic day (E)8.5, the strongest staining was observed in the neural tube. At E11.5 and E13.5, staining was detectable in all parts of the embryo and was particularly notable in the dorsal root ganglia and the inter-digit region of limb buds. At E18.5, staining was evident in nearly all tissues, with skin, bones, and the gastrointestinal tract exhibiting high levels of staining.

To assess the effect of SREBP-2 deficiency during development, we analyzed embryos at multiple developmental stages. *Srebf2*^{−/−} embryos died between E12.5 and E14.5 (Fig. 1D). At E12.5, the *Srebf2*^{−/−} embryos harbored a limb phenotype, with malformed fore- and hindlimbs and impaired digit formation (Fig. 1D). The blood vessels within the limbs appeared dilated, and these regions became necrotic prior to embryonic death.

Altered limb patterning gene expression in SREBP-2-deficient embryos

The malformed limbs in *Srebf2*^{−/−} embryos suggested that SREBP-2 is required for limb patterning. There are two primary signaling centers in the early limb bud: the zone of polarizing activity (ZPA) and the apical ectodermal ridge (AER) (30, 31). They are the source of diffusible morphogens that control spatial patterning. Activities of the ZPA and AER are coordinated through a feedback regulatory circuit dependent on sonic hedgehog (SHH) and fibroblast growth factors (FGFs) (32–36). Additional morphogens, such as gremlin 1 (*Grem1*) and bone morphogenetic proteins (BMPs), are critical for propagating the SHH signal from the ZPA and for inducing FGF signaling in the AER (31). SHH signaling, along with the reciprocal positive interaction between the AER and ZPA, are crucial for regulating limb bud outgrowth, axial patterning, and digit number (32).

We assessed the expression of ZPA and AER patterning genes with whole-mount in situ hybridization on embryos. We selected embryos at E11.5, at which time the ZPA/AER pathways are active, but limb developmental defects in SREBP-2-deficient embryos are not yet visible. As expected, *Shh* expression was present exclusively in the ZPA and *Shh* was expressed at higher levels in *Srebf2*^{−/−} compared with WT embryos (Fig. 2). Expression of the SHH receptor, patched 1 (*Ptch1*), was reduced in forelimbs and hindlimbs of *Srebf2*^{−/−} embryos (compared with WT embryos). During development, activation of *Ptch1* by SHH leads to the release of the smoothed (Smo) receptor and induction of the Gli1 transcription factor, which activates target genes such as *Bmp4*. The *Srebf2*^{−/−} embryos exhibited alterations in some, but not all, of these genes in the SHH signaling axis. Although levels of *Gli1* mRNA were not substantially altered in *Srebf2*^{−/−} embryos, the *Gli1* target gene, *Bmp4*, was expressed at reduced levels in *Srebf2*^{−/−} limb buds, but increased expression in the developing brain and spinal cord. *Bmp5* expression was elevated and *Fgf8* expression was unchanged in *Srebf2*^{−/−} embryos. These results indicate that lack of SREBP-2 in the developing embryo leads to abnormal regulation of some genes involved in limb bud morphogenesis.

To further explore the role of SREBP-2 and cholesterol homeostasis during embryonic development, we generated MEFs from E11.5 WT and *Srebf2*^{−/−} embryos and assessed expression of ZPA genes. Examination of marker genes for the AER signaling cascade in MEFs revealed striking effects of *Srebf2* deficiency on the expression of key morphogens (*Grem1*, *Bmp2*, *Bmp4*, *Fgf8*). *Srebf2*^{−/−} caused marked reductions in the expression of *Grem1*,

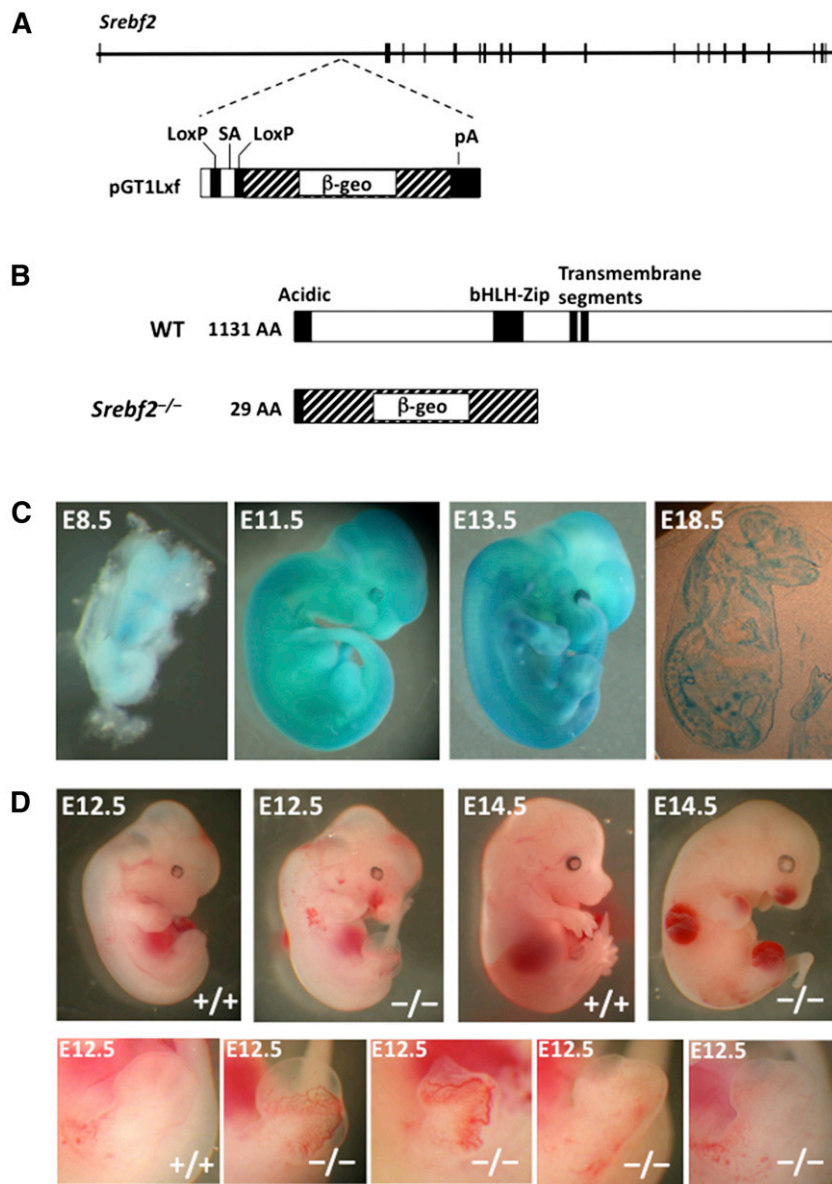


Fig. 1. Generation of SREBP-2-deficient mice. A: Gene-trap vector location in intron 1 of *Srebf2*. SA, splice acceptor; pA, polyadenylation signal. B: Representation of WT SREBP-2 and the SREBP-2- β -geo fusion protein generated from the gene-trap allele. The number of SREBP-2 amino acids (AA) is noted on the left. Most of the SREBP-2 protein sequences are absent from the fusion protein, including the NH₂-terminal DNA-binding domain, the transmembrane domains, and the carboxyl-terminal regulatory domain. C: β -Galactosidase staining of embryos at indicated stages of development. D: *Srebp2*^{-/-} embryos at E12.5 and E14.5 with close-up views of the limbs.

Bmp4, and *Fgf8* and a 4-fold increase in *Bmp2* expression (Fig. 3). The reduction of *Fgf8* levels in MEFs was different from the normal levels of expression in *Srebf2*^{-/-} embryos (Fig. 2), suggesting that some compensatory adjustments in gene expression may occur in vivo. Expression of another developmental gene, *Hoxd13*, was not affected by *Srebf2* deficiency (Fig. 3). These findings implicate SREBP-2 in the regulation of AER morphogen gene expression, either directly or indirectly. We next assessed the effects of cholesterol deprivation on ZPA and AER gene expression. MEFs were treated with a combination of mevinoxin (to suppress cholesterol biosynthesis), β -cyclodextrin (to deplete cellular cholesterol content), and charcoal-treated

serum (to reduce exogenous cholesterol in the medium). Sterol deprivation in MEFs had similar effects as *Srebf2* deficiency: *Bmp2* gene expression was induced, whereas *Bmp4* and *Fgf8* were downregulated (Fig. 3). These results indicate that SREBP-2 and cellular cholesterol homeostasis have a role in regulating limb development-related genes.

SREBP-2 is critical for embryonic hepatic lipid homeostasis

To assess the role of SREBP-2 on cholesterol homeostasis in the liver during embryonic development, we collected embryos at E11.5 and assessed expression of *Srebf*

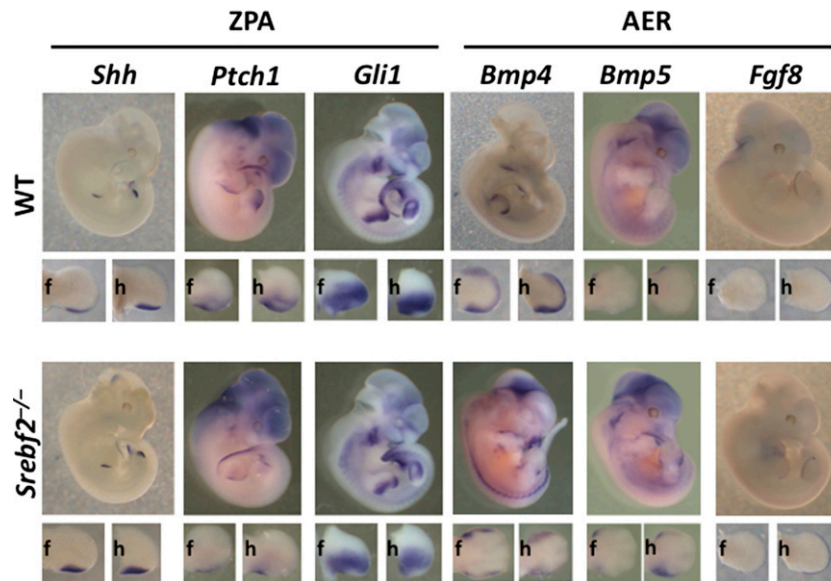


Fig. 2. Whole-mount in situ hybridization. Expression of genes involved in the ZPA (*Shh*, *Ptch1*, *Gli1*) and the AER (*Bmp4*, *Bmp5*, *Fgf8*) at E11.5 are shown. Close-up views of forelimbs (f) and hindlimbs (h) are shown below each embryo. *Srebf2*^{-/-} embryos had increased *Shh* and *Bmp5* expression along with reduced *Ptch1*, *Gli1*, and *Bmp4* expression. *Fgf8* expression levels in WT and *Srebf2*^{-/-} embryos were similar.

and its target genes in the liver; we also extracted lipids from the remainder of the embryo. Whole body cholesterol and triglyceride levels were similar in WT and *Srebf2*^{-/-} embryos (Fig. 4A). As expected, *Srebf2* mRNA levels in liver were nearly undetectable, and target genes involved in cholesterol synthesis [HMG-CoA synthase (*Hmgcs*), HMG-CoA reductase (*Hmgcr*), SREBP protein processing (*Insig1*), and cellular cholesterol uptake [LDL receptor (*Ldlr*)] were significantly reduced (Fig. 4B). Also reduced by 70–80% were *Srebf1a* and *Srebf1c* transcript levels (Fig. 4C), consistent with a feed-forward regulatory loop between SREBP-2 and SREBP-1c (37, 38). We also found reduced transcripts for SREBP1-regulated fatty acid synthesis genes [acetyl-CoA carboxylase (*Acc*), *Fasn*, stearoyl-CoA desaturase 1 (*Scd1*)] (Fig. 4B). Thus, *Srebf2*-deficient embryos displayed reduced expression of both SREBP-1c and SREBP-2 target genes.

Reduced fat reserves in an adult SREBP-2-deficient mouse

We recovered one viable *Srebf2*^{-/-} mouse from a total of ~200 progeny from *Srebf2*^{+/-} × *Srebf2*^{+/-} intercrosses. At 2 months of age, the SREBP-2-deficient mouse was hairless and weighed 40% less than its littermates (Fig. 5A). *Srebf2* deficiency was confirmed by an absence of SREBP-2 protein in the liver (Fig. 5B). The size of the liver was similar to that of heterozygous littermates when normalized to body weight (Fig. 5C). The *Srebf2*^{-/-} mouse had dramatically reduced fat reserves, with nearly undetectable gonadal white adipose tissue (WAT) and markedly reduced inguinal subcutaneous WAT mass (Fig. 5C). Histological examination of tissue harvested from the perigonadal fat pad revealed smaller adipocytes with reduced lipid accumulation (Fig. 5D, top). Sections through the skin showed strata of dermal, adipose, and

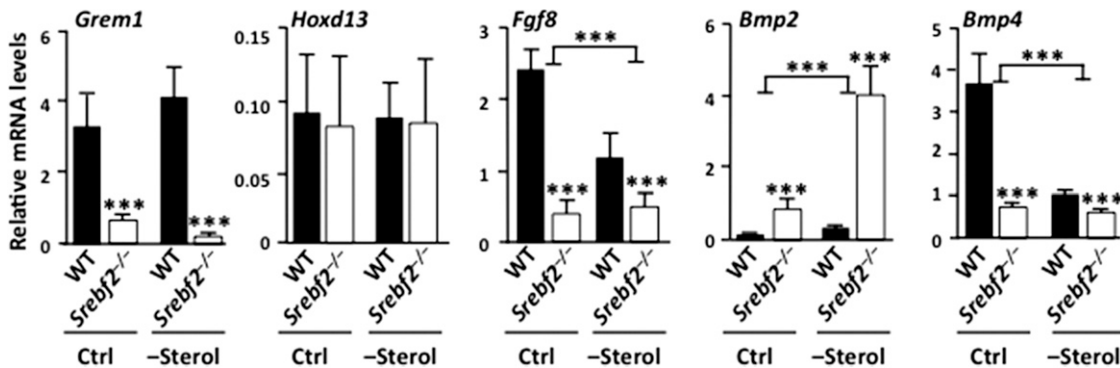


Fig. 3. Effect of SREBP-2 deficiency and sterol depletion on gene expression. WT and *Srebf2*^{-/-} MEFs were cultured under control (Ctrl) conditions (DMEM with 10% FBS) or sterol-depleted conditions (-Sterol) [DMEM with 10% charcoal-stripped FBS, 0.5% (2-hydroxypropyl)- β -cyclodextrin, 20 μ M mevastatin]. RNA was isolated after an overnight incubation, and transcript levels were quantitated by qPCR. Data represent the mean \pm SD (n = 6). ****P* < 0.001 by two-way ANOVA.

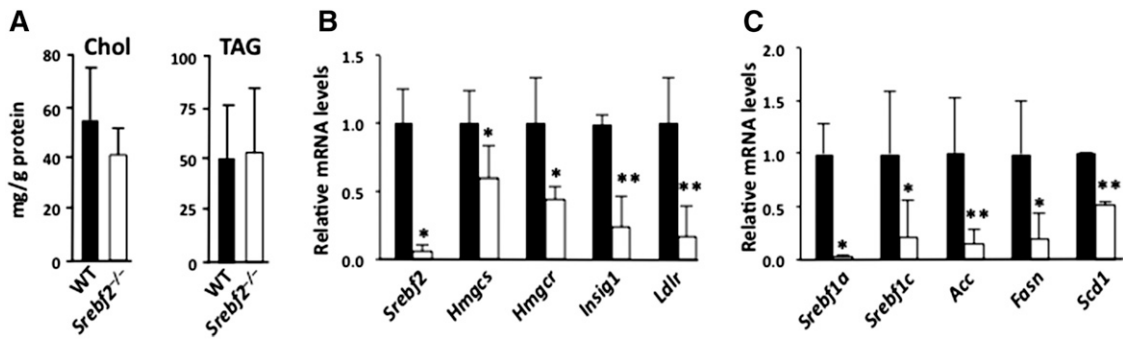


Fig. 4. Lipid levels and gene expression in *Srebf2*^{-/-} embryos. A: Cholesterol (Chol) and triacylglycerol (TAG) levels in E11.5 whole embryos. Expression levels of steroidogenic-related (B) and fatty acid synthesis-related (C) genes in liver of E11.5 embryos. All WT values are set at 1. Data represent the mean \pm SD (n = 4). **P* < 0.05, ***P* < 0.01 versus WT. *Mvk*, mevalonate kinase.

muscle tissue in WT mice, but subdermal adipose tissue was virtually undetectable in the *Srebf2*^{-/-} mouse (Fig. 5D, bottom). Even though limb bud abnormalities were encountered in *Srebf2*^{-/-} embryos, the skeleton of the sole surviving *Srebf2*^{-/-} mouse appeared normal (Fig. 5E).

The single adult *Srebf2*^{-/-} mouse provided an opportunity to assess effects of SREBP-2 deficiency on liver and adipose tissue lipids and on gene expression levels. The effects of *Srebf2* deficiency in adult liver mirrored those observed in *Srebf2*^{-/-} embryos. Although statistical analysis was not possible due to availability of only a single

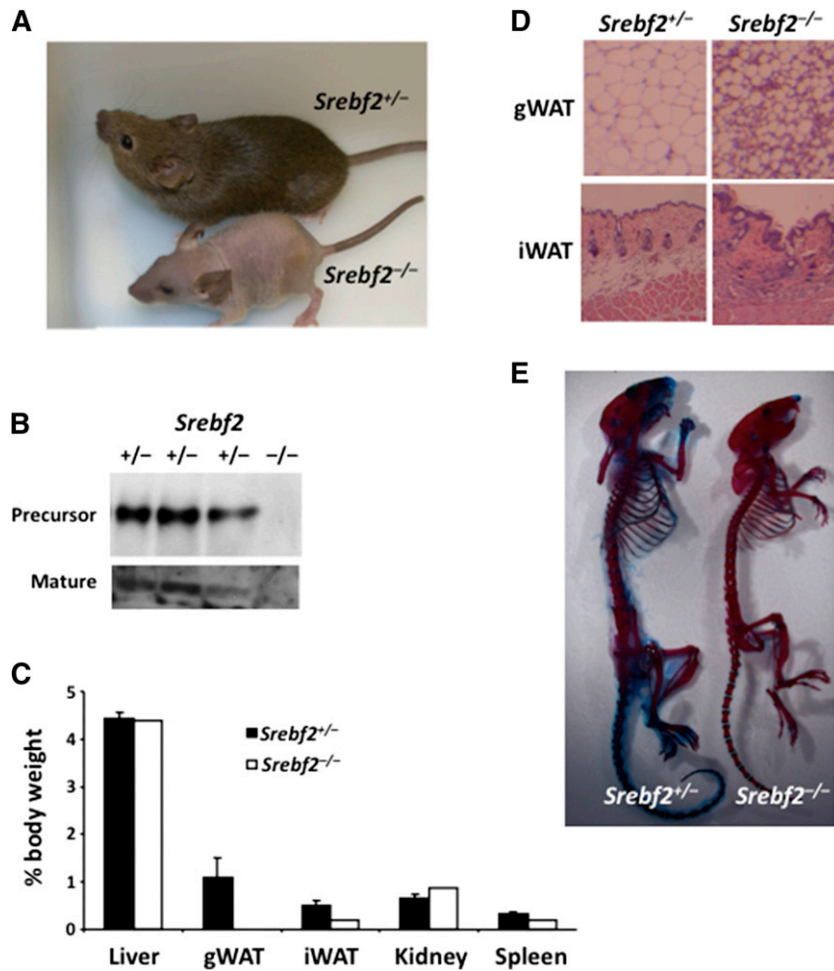


Fig. 5. Characterization of an adult *Srebf2*^{-/-} mouse. A: Photo of the 2-month-old *Srebf2*^{-/-} mouse with a *Srebf2*^{+/-} littermate. B: Immunoblot analysis of SREBP-2 from livers of *Srebf2*^{+/-} and *Srebf2*^{-/-} mice. C: Percent body weight of liver, gonadal WAT (gWAT), inguinal WAT (iWAT), kidney, and spleen. D: Hematoxylin/eosin staining of gWAT and iWAT. E: Alizarin red (bone) and Alcian blue (cartilage) staining of the skeleton.

Srebf2^{-/-} mouse, hepatic cholesterol levels in the *Srebf2*^{-/-} mouse were reduced by 40% and triacylglycerol levels were reduced by 60% (Fig. 6A). Transcript levels for *Srebf1a* and *Srebf1c* in the liver were reduced, as were the transcripts for most SREBP target genes analyzed (Fig. 6B). In inguinal WAT, cholesterol levels were reduced by approximately one-half compared with heterozygous littermates, but triacylglycerol levels (normalized to protein) were similar (Fig. 6C). In contrast to the liver of the *Srebf2*^{-/-} mouse, most SREBP target genes in WAT were expressed at levels similar to those in WT mice (Fig. 6D). Interestingly, *Srebf1a* mRNA levels in WAT were elevated 5-fold, whereas *Srebf1c* mRNA levels were normal. In addition, the expression levels for *Acc*, *Fasn*, and *Scd1* were equal to (or exceeded) those in *Srebf2*^{+/-} mice. Thus, in the adipose tissue of the *Srebf2*^{-/-} mouse, higher levels of *Srebf1a* expression may have partially compensated for the loss of SREBP-2.

Srebf2 hypomorphic mice exhibit reduced adiposity and sex-specific lethality as young adults

While we were able to study a single viable *Srebf2*^{-/-} mouse, embryonic lethality prevented us from thoroughly investigating SREBP-2 function in adult mice. To circumvent this issue, we used *Cre* recombinase to remove the splice acceptor in the gene-trap allele, with the goal of restoring limited amounts of normal mRNA splicing and creating mice with a hypomorphic *Srebf2* allele (*Srebf2*^{hyp}). Intercrosses of *Srebf2*^{+/-} and *Srebf2*^{+ /hyp} mice generated 127 live offspring, 19% of which (compared with 25% expected)

were compound heterozygotes for the hypomorphic and null alleles (*Srebf2*^{/hyp}). Hepatic SREBP-2 protein levels in the *Srebf2*^{/hyp} mice were 80–90% lower than in WT mice (Fig. 7B). *Srebf2*^{/hyp} mice appeared grossly normal during the neonatal period, but the females had reduced body weight beginning at 4 weeks of age (Fig. 7C), and 50% of these animals died between 8 and 12 weeks of age (Fig. 7D). Male *Srebf2*^{/hyp} mice exhibited normal body weight and survived until the study was terminated at 12 weeks of age. Compared with WT mice, male *Srebf2*^{/hyp} mice had 20–40% lower fat pad tissue mass and 15% lower liver mass (relative to total body weight) (Fig. 7E).

We hypothesized that impaired steroid hormone synthesis might contribute to lethality in female *Srebf2*^{/hyp} mice. However, our analyses of hormone levels did not reveal a likely cause of the premature death in females. Plasma estradiol and progesterone levels were normal in females. Male *Srebf2*^{/hyp} mice actually had elevated levels of aldosterone and corticosterone in the plasma (Table 1).

Effects of reduced *Srebf2* gene expression in liver and adipose tissue

We studied adult *Srebf2*^{/hyp} mice to assess effects of reduced SREBP-2 expression on cholesterol homeostasis. At 12 weeks of age, *Srebf2*^{/hyp} males had reduced cholesterol levels in the liver, but not in adipose tissue; tissue triacylglycerol levels were normal (Fig. 8A, C). Reduced SREBP-2 expression also led to lower expression of cholesterol biosynthetic and lipogenic genes in the liver (Fig. 8B), but not in adipose tissue (Fig. 8D). *Srebf2*^{/hyp} mice had reduced

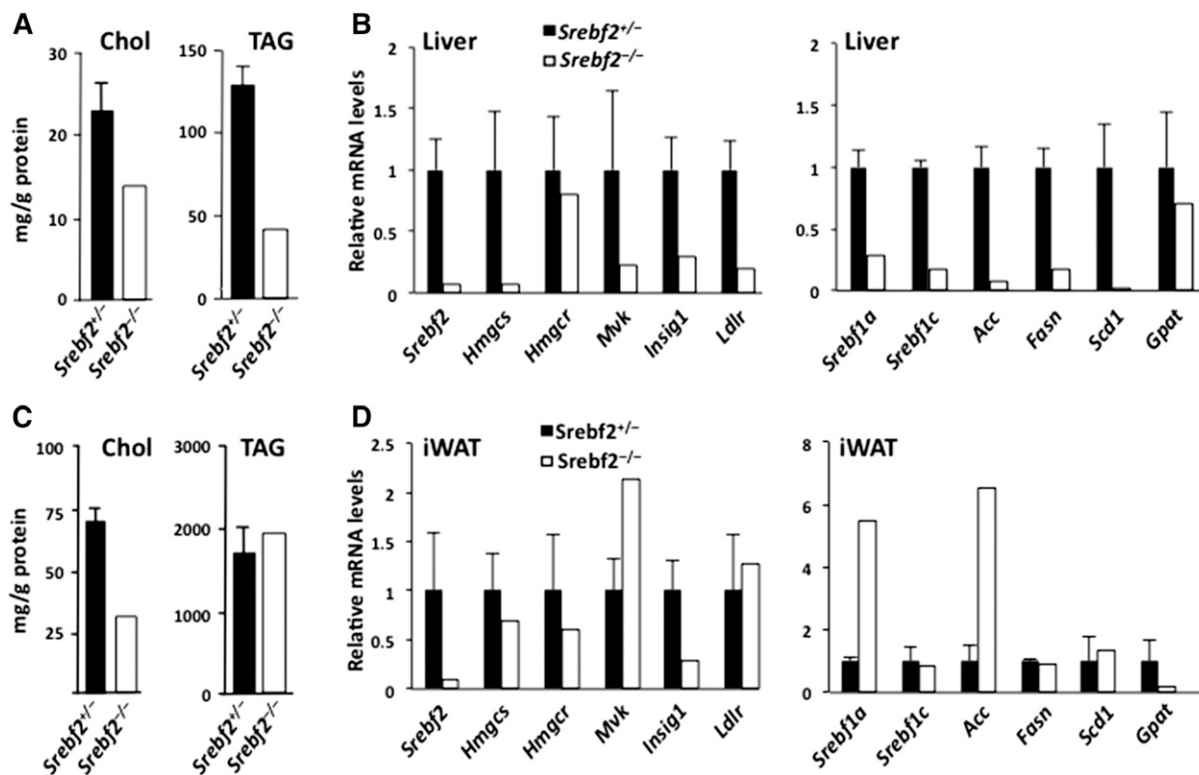


Fig. 6. Lipid levels and gene expression in the liver and WAT of the viable *Srebf2*^{-/-} mouse. Cholesterol (Chol) and triacylglycerol (TAG) levels in liver (A) and inguinal (i)WAT (C). mRNA levels in liver (B) and iWAT (D) of the adult *Srebf2*^{-/-} mouse. All control (*Srebf2*^{+/-}) values are set to 1. Data represent the mean ± SD (n = 3 for *Srebf2*^{+/-} and n = 1 for *Srebf2*^{-/-}).

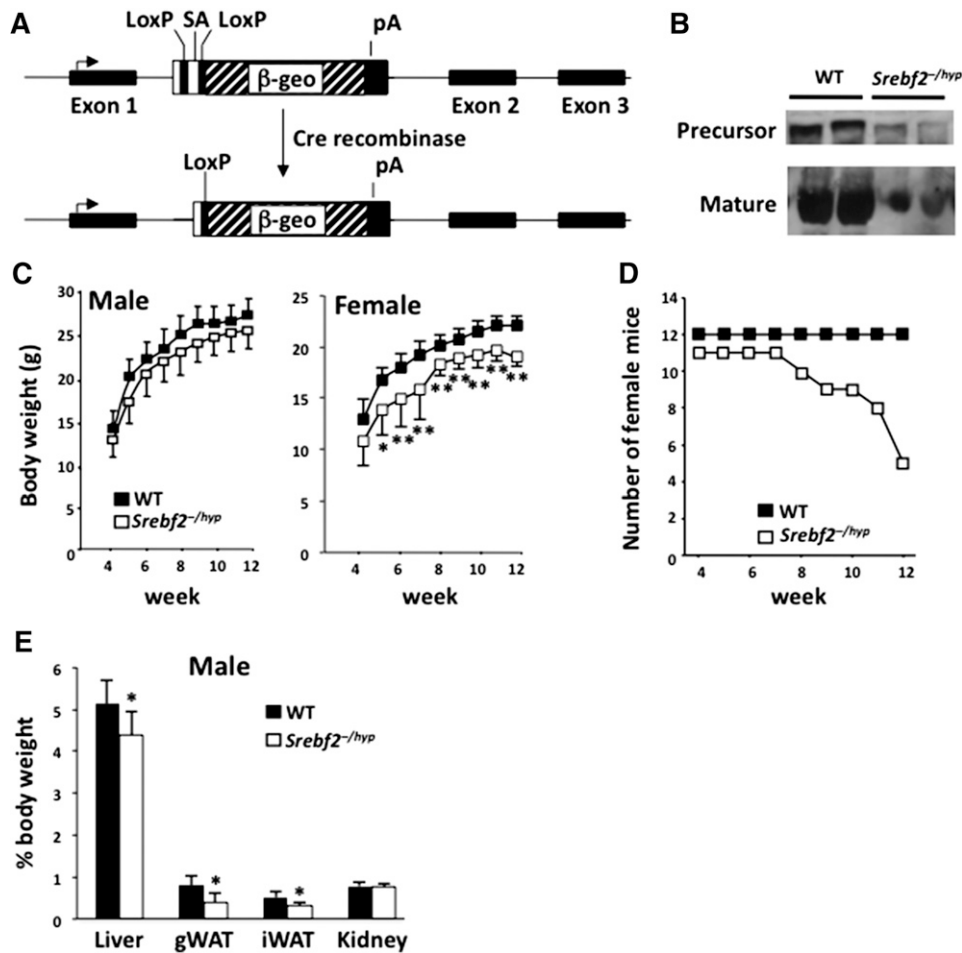


Fig. 7. Characterization of mice carrying a hypomorphic *Srebf2* allele. A: Schematic representation of the *Srebf2* mutant allele before and after removal of the floxed splice acceptor (SA) sequences with an *Hprt-Cre* transgene. pA, polyadenylation signal. B: SREBP-2 protein levels in liver. C: Weight gain in male and female *Srebf2*^{-hyp} mice during the first 12 weeks. D: Survival of female *Srebf2*^{-hyp} mice from 4 to 12 weeks of age. Females, but not males, had a reduced life-span (n = 11–12 mice per group). E: Percent body weight of liver, gonadal (g)WAT, inguinal (i)WAT, and kidney in male *Srebf2*^{-hyp} mice. C, E: Mean ± SD (n = 6 per group).

Srebf1 gene expression, with 90% lower *Srebf1c* mRNA levels in liver and 70% lower *Srebf1c* levels in adipose tissue. *Srebf1a* levels were modestly altered in both tissues (Fig. 8B, D). The adipose tissue of *Srebf2*^{-hyp} mice displayed a 6-fold increase in transcripts for the LDL receptor (Fig. 8D). Given that the gene for miR-33a resides within an intron of *Srebf2*, we assessed whether the *Srebf2* gene-trap allele leads to altered miR-33a mRNA expression. miR-33a RNA levels and mRNA levels for several miR-33a target genes were similar in livers of *Srebf2*^{-hyp} and WT mice (Fig. 8E, F). Glucose-6-phosphatase (*G6pc*) mRNA levels were decreased in the hypomorphic mice, but because miR-33a and other target genes tested were expressed at WT levels, this is unlikely a result of altered miR-33a regulation.

The gene expression patterns in tissues of *Srebf2*^{-/-} and *Srebf2*^{-hyp} mice could have been influenced by secondary compensatory responses. To verify the effects of SREBP-2 deficiency on gene expression, we assessed basal gene expression and sterol regulation of gene expression in *Srebf2*^{-/-} MEFs. Under basal conditions (DMEM with 10% FBS; shown in the left two bars of each graph), several cholesterol biosynthetic genes [*Hmgcs*, *Hmgcr*, mevalonate kinase (*Mvk*)] and *Ldlr* were expressed at significantly lower levels in the *Srebf2*^{-/-} MEFs (Fig. 9A), mirroring the gene expression findings in the liver of *Srebf2*^{-hyp} mice (Fig. 8B). SREBP-2 deficiency in MEFs led to nearly undetectable *Srebf1c* mRNA levels, but to increased levels of *Srebf1a* transcripts (Fig. 9B). SREBP-2 deficiency also

TABLE 1. Plasma steroid hormone levels

Genotype	Female		Male		
	Estradiol (pg/ml)	Progesterone (ng/ml)	Aldosterone (pg/ml)	Corticosterone (ng/ml)	Testosterone (ng/ml)
<i>Srebf2</i> ^{+/+}	15.7 ± 5.5	15.4 ± 10.6	569 ± 434	466 ± 291	2.8 ± 5.2
<i>Srebf2</i> ^{-hyp}	12.3 ± 3.1	12.4 ± 2.2	1,554 ± 253	863 ± 293	1.1 ± 1.2
t-test	NS	NS	P < 0.05	P < 0.05	NS

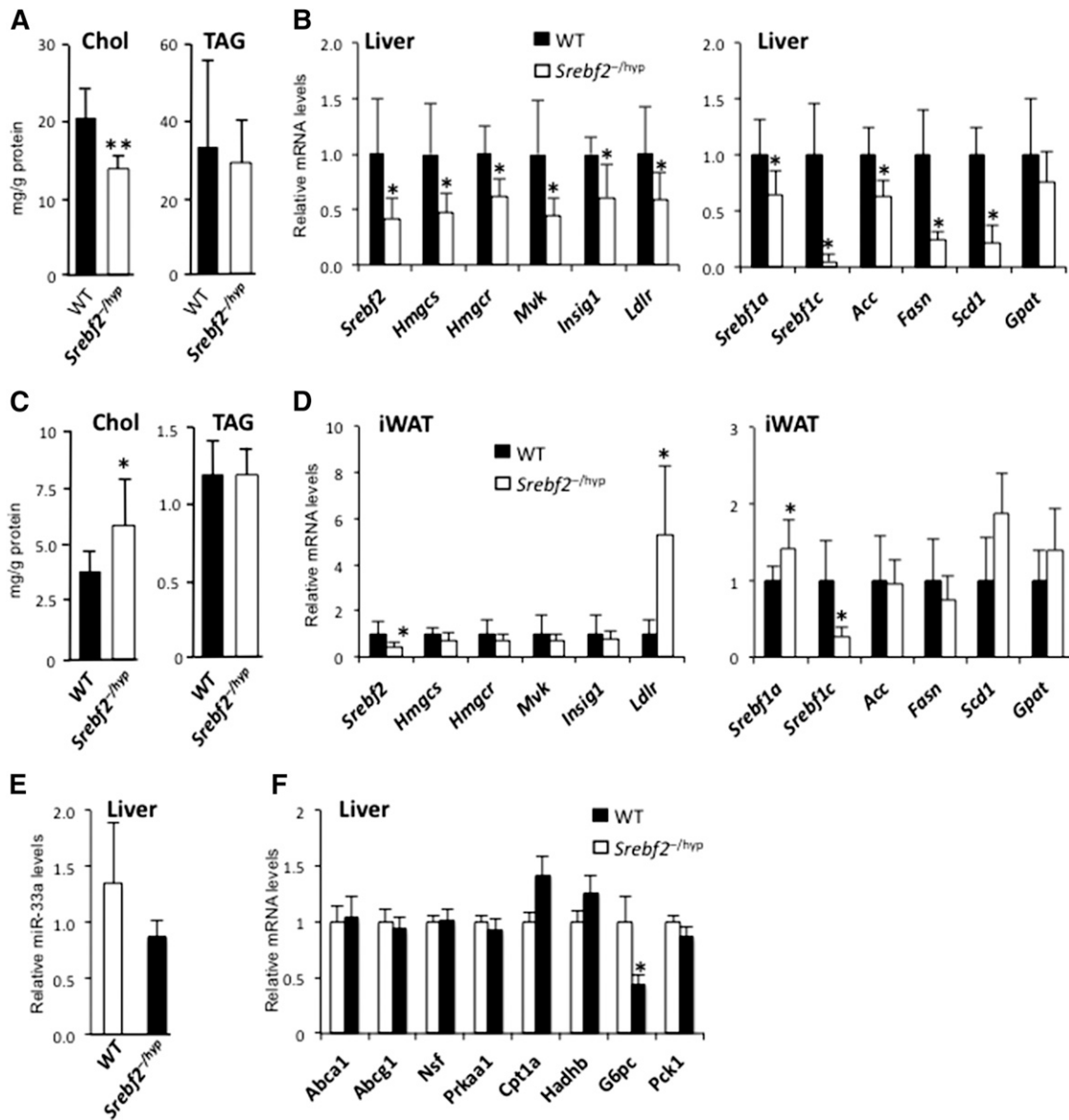


Fig. 8. Lipid levels and gene expression in the liver and inguinal (i)WAT of *Srebf2*^{-/-hyp} mice. Cholesterol and triacylglycerol (TAG) levels in liver (A) and iWAT (C) of *Srebf2*^{-/-hyp} mice. mRNA levels in liver (B) and iWAT (D) of *Srebf2*^{-/-hyp} mice. Hepatic levels of miR-33a (E) and mRNA for several target genes (F). All WT values are set to 1.0. Data represent mean \pm SD (n = 6 per group). **P* < 0.05 versus WT. *Nsf*, N-ethylmaleimide-sensitive factor; *Prkaa1*, AMP-activated protein kinase α 1 catalytic subunit; *Cpt1a*, carnitine palmitoyltransferase 1a; *Hadhb*, hydroxyacyl-CoA dehydrogenase/3-ketoacyl-CoA thiolase/enoyl-CoA hydratase β subunit; *G6pc*, glucose-6-phosphatase; *Pck1*, phosphoenolpyruvate carboxykinase-1.

impaired the regulation of gene expression in response to sterol deprivation, with a failure to induce SREBP target genes, with the exception of *Srebf1a* (Fig. 9, the two bars at the right of each panel). Thus, SREBP-2 is required for basal expression of *Srebf1c*, but not *Srebf1a*, and also is essential for sterol regulation of many SREBP target genes.

DISCUSSION

It has long been appreciated that SREBP-2 is a crucial transcriptional regulator of lipid homeostasis. SREBP-1 and SREBP-2 preferentially target genes involved in fatty

acid synthesis and cholesterol biosynthesis, respectively (7). However, the activities of the two transcription factors overlap, making it challenging to decipher their unique physiological functions. Previously published studies characterized effects of SREBP-1 deficiency in the mouse (14), but the impact of SREBP-2 deficiency was not characterized. Here, we used a combination of two mutant *Srebf2* alleles to investigate the roles of SREBP-2 in mouse development and in adult mice. We identified a crucial role for SREBP-2 in survival and in limb patterning through effects on the SHH pathway. We also demonstrated a key role for SREBP-2 in maintaining hepatic cholesterol content and in regulating *Srebf1* gene expression, in addition to regulating well-established SREBP-2 target genes.

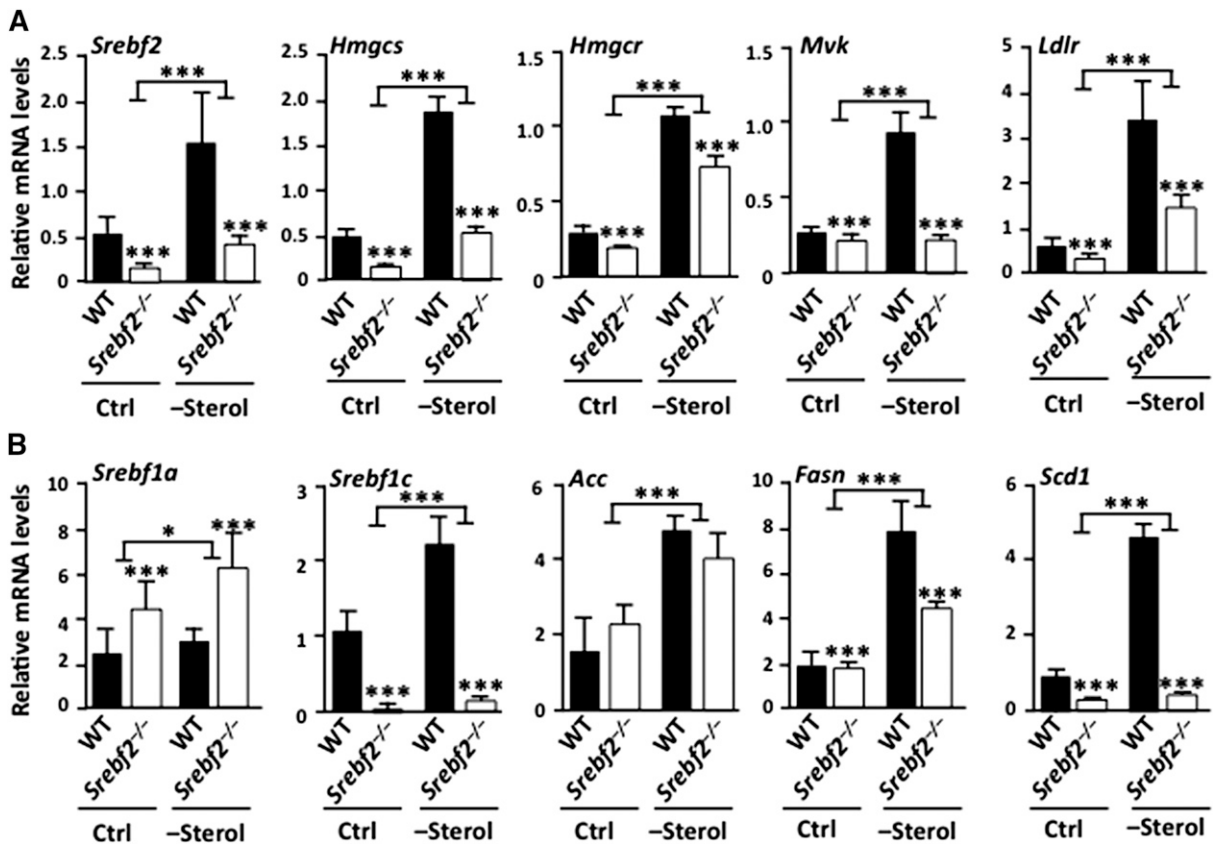


Fig. 9. Effect of SREBP-2 deficiency and sterol depletion on gene expression. WT and *Srebf2*^{-/-} MEFs were cultured under control conditions (DMEM with 10% FBS) or sterol-depleted conditions [DMEM with 10% charcoal-stripped FBS, 0.5% (2-hydroxypropyl)- β -cyclodextrin, 20 μ M mevastatin]. RNA was isolated after an overnight incubation and mRNA levels were determined by qPCR. Data represent mean \pm SD (n = 6 per group). * P < 0.05; *** P < 0.001 by two-way ANOVA.

SREBP-2 deficiency is incompatible with normal embryonic development; most *Srebf2*^{-/-} embryos died by 14.5 days post coitus. This finding likely explains why no one has encountered or studied a human subject with complete SREBP-2 deficiency. In the mouse, a spontaneous *Srebf2* missense mutation was associated with cataracts and persistent skin wounds (39), but the effect of the amino acid substitution on SREBP-2 activity is unknown, but unlikely to abolish activity. The cause of death in *Srebf2*^{-/-} embryos is unclear, given that *Srebf2* expression is expressed widely and multiple organ systems could have been compromised by the absence of SREBP-2.


A striking phenotype of *Srebf2*^{-/-} embryos was abnormal digit formation. At 13.5 days post coitus, *Srebf2* expression is detectable in the limb buds of WT embryos in the regions destined to undergo apoptosis during digit specification. The absence of digit formation in *Srebf2*^{-/-} embryos confirmed a requirement for SREBP-2 in this process. This finding is in accord with previous work showing that in the developing limb bud, there is spatial concordance between cholesterol biosynthetic gene activity and the apoptotic process that defines the digits (40). Gene expression analyses in *Srebf2*^{-/-} embryos revealed alterations in pathways that regulate limb morphogenesis, including components of the SHH signaling axis. Limb buds of *Srebf2*^{-/-} embryos exhibited increased *Shh* transcript level, but

reduced expression of downstream components of the signaling pathway (*Ptch1*, *Bmp4*). Given that both SHH and *Ptch1* both contain sterol-sensing domains (41), it is interesting to speculate that SREBP-2 regulation of cholesterol levels in the developing embryo may play a role in the proper functioning of this pathway, but additional work is required.

Our results in the *Srebf2*^{hyp} mice demonstrate that low levels of SREBP-2 expression are sufficient for survival during embryogenesis. *Srebf2*^{hyp} mice are born at a near-normal frequency; the viability of males appeared normal, but the females exhibited failure-to-thrive and most succumbed during the first few months of life. An analysis of steroid hormones was not helpful in explaining the differences in the survival of males and females. Studies of adult male *Srebf2*^{hyp} mice revealed a complex relationship between *Srebf2* expression and the regulation of *Srebf1*. Previous work established that loss of SREBP-1 leads to increased hepatic SREBP-2 transcript and protein levels, increased expression of cholesterol biosynthetic genes, and a 3-fold increase in hepatic cholesterol content (14). We found that reduced SREBP-2 expression in *Srebf2*^{hyp} mice resulted in tissue-specific alterations in *Srebf1* expression. In the liver, the *Srebf2*^{hyp} mice had nearly undetectable levels of *Srebf1c* transcripts and an 80% reduction in *Srebf1a* transcripts. The low levels of SREBPs in these mice were accompanied by

40% lower stores of cholesterol in the liver. In contrast, the cholesterol content of adipose tissue and embryonic fibroblasts was maintained despite a 70% reduction in *Srebf1c* expression, perhaps because of slightly increased *Srebf1a* expression levels.

Exon 16 of *Srebf2* encodes a microRNA, miR-33a, which appears to be generated as a result of mRNA splicing following transcription of the *Srebf2* gene (42–45). miR-33a targets transcripts from multiple genes involved in cellular cholesterol efflux, such as *Abcg1* and *Abcg1*, and miR-33a inhibition has been proposed as an anti-atherosclerosis treatment (46, 47). It is thought that the coordinate expression of *Srebf2* and miR-33a represents a mechanism to maintain cellular cholesterol homeostasis by enhancing cholesterol synthesis while limiting sterol efflux. Because miR-33a is present within the *Srebf2* locus, it was possible that miR-33a levels would be reduced in our *Srebf2*-deficient mice. However, the expression of miR-33a and several target genes were not perturbed in the liver, suggesting that the *Srebf2* mutant allele did not disrupt miR-33a expression. Furthermore, the phenotypes of our mice did not recapitulate those of miR-33a-deficient mice, which manifest hepatic steatosis and are prone to increased body weight on chow and high-fat diets (48). It is possible that miR-33a production is unaffected by our gene-trapped alleles or that there are compensatory changes in our mice that serve to maintain transcript levels for miR-33a target genes.

Finally, these studies provide a proof-of-principle for generation of hypomorphic alleles from gene-trap insertions. Gene trapping has been a valuable adjunct to standard homologous recombination approaches for deciphering gene function in mice (21, 22). Regardless of which technique is used, it is often the case that knocking out a gene in mice results in lethality during embryonic development. In those cases, most investigators rely on the production of tissue-specific knockout mice to assess gene function. In the current study, we showed that the creation of a hypomorphic allele from the gene-trap insertion represents a useful approach for deciphering gene function. We used Cre recombinase to remove the slice acceptor site in the gene-trap allele, which restored a low level of *Srebf2* transcripts and led to markedly reduced SREBP-2 levels throughout the body. Of note, this approach is not limited to creating a “global hypomorphic mouse;” it would have been possible to use a cell type-specific Cre transgene to create mice that express low amounts of SREBP-2 in a tissue. 

The authors thank Lise Zakin for helpful discussions regarding in situ hybridizations.

REFERENCES

- Lingwood, D., and K. Simons. 2010. Lipid rafts as a membrane-organizing principle. *Science*. **327**: 46–50.
- Maxfield, F. R., and G. van Meer. 2010. Cholesterol, the central lipid of mammalian cells. *Curr. Opin. Cell Biol.* **22**: 422–429.
- Horton, J. D., J. L. Goldstein, and M. S. Brown. 2002. SREBPs: activators of the complete program of cholesterol and fatty acid synthesis in the liver. *J. Clin. Invest.* **109**: 1125–1131.
- Jeon, T.-I., and T. F. Osborne. 2012. SREBPs: metabolic integrators in physiology and metabolism. *Trends Endocrinol. Metab.* **23**: 65–72.
- Ye, J., and R. A. DeBose-Boyd. 2011. Regulation of cholesterol and fatty acid synthesis. *Cold Spring Harb. Perspect. Biol.* **3**: a004754.
- Pai, J. T., O. Guryev, M. S. Brown, and J. L. Goldstein. 1998. Differential stimulation of cholesterol and unsaturated fatty acid biosynthesis in cells expressing individual nuclear sterol regulatory element-binding proteins. *J. Biol. Chem.* **273**: 26138–26148.
- Horton, J. D., N. A. Shah, J. A. Warrington, N. N. Anderson, S. W. Park, M. S. Brown, and J. L. Goldstein. 2003. Combined analysis of oligonucleotide microarray data from transgenic and knockout mice identifies direct SREBP target genes. *Proc. Natl. Acad. Sci. USA*. **100**: 12027–12032.
- McPherson, R., and A. Gauthier. 2004. Molecular regulation of SREBP function: the Insig-SCAP connection and isoform-specific modulation of lipid synthesis. *Biochem. Cell Biol.* **82**: 201–211.
- Shimano, H., J. D. Horton, I. Shimomura, R. E. Hammer, M. S. Brown, and J. L. Goldstein. 1997. Isoform 1c of sterol regulatory element binding protein is less active than isoform 1a in livers of transgenic mice and in cultured cells. *J. Clin. Invest.* **99**: 846–854.
- Goldstein, J. L., R. A. DeBose-Boyd, and M. S. Brown. 2006. Protein sensors for membrane sterols. *Cell*. **124**: 35–46.
- Goldstein, J. L., and M. S. Brown. 2015. A century of cholesterol and coronaries: from plaques to genes to statins. *Cell*. **161**: 161–172.
- Horton, J. D., I. Shimomura, M. S. Brown, R. E. Hammer, J. L. Goldstein, and H. Shimano. 1998. Activation of cholesterol synthesis in preference to fatty acid synthesis in liver and adipose tissue of transgenic mice overproducing sterol regulatory element-binding protein-2. *J. Clin. Invest.* **101**: 2331–2339.
- Shimano, H., J. D. Horton, R. E. Hammer, I. Shimomura, M. S. Brown, and J. L. Goldstein. 1996. Overproduction of cholesterol and fatty acids causes massive liver enlargement in transgenic mice expressing truncated SREBP-1a. *J. Clin. Invest.* **98**: 1575–1584.
- Shimano, H., I. Shimomura, R. E. Hammer, J. Herz, J. L. Goldstein, M. S. Brown, and J. D. Horton. 1997. Elevated levels of SREBP-2 and cholesterol synthesis in livers of mice homozygous for a targeted disruption of the SREBP-1 gene. *J. Clin. Invest.* **100**: 2115–2124.
- Yang, J., J. L. Goldstein, R. E. Hammer, Y. A. Moon, M. S. Brown, and J. D. Horton. 2001. Decreased lipid synthesis in livers of mice with disrupted Site-1 protease gene. *Proc. Natl. Acad. Sci. USA*. **98**: 13607–13612.
- Matsuda, M., B. S. Korn, R. E. Hammer, Y. A. Moon, R. Komuro, J. D. Horton, J. L. Goldstein, M. S. Brown, and I. Shimomura. 2001. SREBP cleavage-activating protein (SCAP) is required for increased lipid synthesis in liver induced by cholesterol deprivation and insulin elevation. *Genes Dev.* **15**: 1206–1216.
- Chevy, F., F. Illien, C. Wolf, and C. Roux. 2002. Limb malformations of rat fetuses exposed to a distal inhibitor of cholesterol biosynthesis. *J. Lipid Res.* **43**: 1192–1200.
- Gofflot, F., C. Hars, F. Illien, F. Chevy, C. Wolf, J. J. Picard, and C. Roux. 2003. Molecular mechanisms underlying limb anomalies associated with cholesterol deficiency during gestation: implications of Hedgehog signaling. *Hum. Mol. Genet.* **12**: 1187–1198.
- Porter, J. A., K. E. Young, and P. A. Beachy. 1996. Cholesterol modification of hedgehog signaling proteins in animal development. *Science*. **274**: 255–259.
- Kanungo, S., N. Soares, M. He, and R. D. Steiner. 2013. Sterol metabolism disorders and neurodevelopment—an update. *Dev. Disabil. Res. Rev.* **17**: 197–210.
- Nord, A. S., P. J. Chang, B. R. Conklin, A. V. Cox, C. A. Harper, G. G. Hicks, C. C. Huang, S. J. Johns, M. Kawamoto, S. Liu, et al. 2006. The International Gene Trap Consortium Website: a portal to all publicly available gene trap cell lines in mouse. *Nucleic Acids Res.* **34**: D642–D648.
- Stryke, D., M. Kawamoto, C. C. Huang, S. J. Johns, L. A. King, C. A. Harper, E. C. Meng, R. E. Lee, A. Yee, L. L’Italien, et al. 2003. BayGenomics: a resource of insertional mutations in mouse embryonic stem cells. *Nucleic Acids Res.* **31**: 278–281.
- Tang, S.-H. E., F. J. Silva, W. M. K. Tsark, and J. R. Mann. 2002. A Cre/loxP-deleter transgenic line in mouse strain 129S1/SvImJ. *Genesis*. **32**: 199–202.
- Vergnes, L., A. P. Beigneux, R. Davis, S. M. Watkins, S. G. Young, and K. Reue. 2006. Agpat6 deficiency causes subdermal lipodystrophy and resistance to obesity. *J. Lipid Res.* **47**: 745–754.

25. Beigneux, A. P., L. Vergnes, X. Qiao, S. Quatela, R. Davis, S. M. Watkins, R. A. Coleman, R. L. Walzem, M. Philips, K. Reue, et al. 2006. Agpat6—a novel lipid biosynthetic gene required for triacylglycerol production in mammary epithelium. *J. Lipid Res.* **47**: 734–744.
26. Zakin, L., and E. M. De Robertis. 2004. Inactivation of mouse Twisted gastrulation reveals its role in promoting Bmp4 activity during forebrain development. *Development.* **131**: 413–424.
27. Zakin, L., B. Reversade, H. Kuroda, K. M. Lyons, and E. M. De Robertis. 2005. Sirenomelia in Bmp7 and Tsg compound mutant mice: requirement for Bmp signaling in the development of ventral posterior mesoderm. *Development.* **132**: 2489–2499.
28. Solloway, M. J., A. T. Dudley, E. K. Bikoff, K. M. Lyons, B. L. Hogan, and E. J. Robertson. 1998. Mice lacking Bmp6 function. *Dev. Genet.* **22**: 321–339.
29. Seo, Y-K., T-I. Jeon, H. K. Chong, J. Biesinger, X. Xie, and T. F. Osborne. 2011. Genome-wide localization of SREBP-2 in hepatic chromatin predicts a role in autophagy. *Cell Metab.* **13**: 367–375.
30. Capdevila, J., and J. C. Izpisua Belmonte. 2001. Patterning mechanisms controlling vertebrate limb development. *Annu. Rev. Cell Dev. Biol.* **17**: 87–132.
31. Bénazet, J-D., and R. Zeller. 2009. Vertebrate limb development: moving from classical morphogen gradients to an integrated 4-dimensional patterning system. *Cold Spring Harb. Perspect. Biol.* **1**: a001339.
32. Cohen, M. M. 2003. The hedgehog signaling network. *Am. J. Med. Genet. A.* **123A**: 5–28.
33. McGlenn, E., and C. J. Tabin. 2006. Mechanistic insight into how Shh patterns the vertebrate limb. *Curr. Opin. Genet. Dev.* **16**: 426–432.
34. Zúñiga, A., A. P. Haramis, A. P. McMahon, and R. Zeller. 1999. Signal relay by BMP antagonism controls the SHH/FGF4 feedback loop in vertebrate limb buds. *Nature.* **401**: 598–602.
35. Verheyden, J. M., and X. Sun. 2008. An Fgf/Gremlin inhibitory feedback loop triggers termination of limb bud outgrowth. *Nature.* **454**: 638–641.
36. Bastida, M. F., R. Sheth, and M. A. Ros. 2009. A BMP-Shh negative-feedback loop restricts Shh expression during limb development. *Development.* **136**: 3779–3789.
37. Sato, R., J. Inoue, Y. Kawabe, T. Kodama, T. Takano, and M. Maeda. 1996. Sterol-dependent transcriptional regulation of sterol regulatory element-binding protein-2. *J. Biol. Chem.* **271**: 26461–26464.
38. Amemiya-Kudo, M., H. Shimano, T. Yoshikawa, N. Yahagi, A. H. Hasty, H. Okazaki, Y. Tamura, F. Shionoiri, Y. Iizuka, K. Ohashi, et al. 2000. Promoter analysis of the mouse sterol regulatory element-binding protein-1c gene. *J. Biol. Chem.* **275**: 31078–31085.
39. Merath, K. M., B. Chang, R. Dubielzig, R. Jeannotte, and D. J. Sidjanin. 2011. A spontaneous mutation in Srebf2 leads to cataracts and persistent skin wounds in the lens opacity 13 (lop13) mouse. *Mamm. Genome.* **22**: 661–673.
40. Laubner, D., R. Breitling, and J. Adamski. 2003. Embryonic expression of cholesterologenic genes is restricted to distinct domains and colocalizes with apoptotic regions in mice. *Brain Res. Mol. Brain Res.* **115**: 87–92.
41. Rahnama, F., R. Toftgård, and P. G. Zaphiropoulos. 2004. Distinct roles of PTCH2 splice variants in Hedgehog signalling. *Biochem. J.* **378**: 325–334.
42. Marquart, T. J., R. M. Allen, D. S. Ory, and A. Baldán. 2010. miR-33 links SREBP-2 induction to repression of sterol transporters. *Proc. Natl. Acad. Sci. USA.* **107**: 12228–12232.
43. Rayner, K. J., Y. Suárez, A. Dávalos, S. Parathath, M. L. Fitzgerald, N. Tamehiro, E. A. Fisher, K. J. Moore, and C. Fernández-Hernando. 2010. MiR-33 contributes to the regulation of cholesterol homeostasis. *Science.* **328**: 1570–1573.
44. Najafi-Shoushtari, S. H., F. Kristo, Y. Li, T. Shioda, D. E. Cohen, R. E. Gerszten, and A. M. Näär. 2010. MicroRNA-33 and the SREBP host genes cooperate to control cholesterol homeostasis. *Science.* **328**: 1566–1569.
45. Tarling, E. J., H. Ahn, and T. Q. de Aguiar Vallim. 2015. The nuclear receptor FXR uncouples the actions of miR-33 from SREBP-2. *Arterioscler. Thromb. Vasc. Biol.* **35**: 787–795.
46. Rayner, K. J., F. J. Sheedy, C. C. Esau, F. N. Hussain, R. E. Temel, S. Parathath, J. M. van Gils, A. J. Rayner, A. N. Chang, Y. Suarez, et al. 2011. Antagonism of miR-33 in mice promotes reverse cholesterol transport and regression of atherosclerosis. *J. Clin. Invest.* **121**: 2921–2931.
47. Horie, T., O. Baba, Y. Kuwabara, Y. Chujo, S. Watanabe, M. Kinoshita, M. Horiguchi, T. Nakamura, K. Chonabayashi, M. Hishizawa, et al. 2012. MicroRNA-33 deficiency reduces the progression of atherosclerotic plaque in ApoE^{-/-} mice. *J. Am. Heart Assoc.* **1**: e003376.
48. Horie, T., T. Nishino, O. Baba, Y. Kuwabara, T. Nakao, M. Nishiga, S. Usami, M. Izuhara, N. Sowa, N. Yahagi, et al. 2013. MicroRNA-33 regulates sterol regulatory element-binding protein 1 expression in mice. *Nat. Commun.* **4**: 2883.